Emerging disease dynamics in a model coupling within-host and between-host systems

Zhilan Feng

Department of Mathematics, Purdue University

Dynamics of Evolution Equations

Luminy, March 21-25, 2016

Application of an SIR model to vaccination policymaking

- An elaboration of theory about preventing outbreaks in homogeneous populations to include heterogeneity or preferential mixing

  Zhilan Feng, Andrew Hill, Philip Smith and John Glasser
  J. Theoretical Biology, 2015

- The effect of heterogeneity in uptake of the measles, mumps, and rubella vaccine on the potential for outbreaks of measles: a modelling study

  John Glasser, Zhilan Feng, Saad Omer, Philip Smith, Lance Rodewald
  Lancet Infectious Diseases, 2016

Accompanied Comment (*Lancet Infectious Diseases*, 2016)

Comment

Managing the risks of vaccine hesitancy and refusals

In *The Lancet Infectious Diseases*, John Glasser and colleagues[1] report the results of a spatially-stratified model to better understand the dynamics of disease outbreaks and the link with vaccine hesitancy and refusal. Using data for 39 132 children starting elementary school in San Diego County, CA, USA, in 2008 (2% of whom had a personal-belief exception to vaccines), the authors show the effect of heterogeneity on the reproduction numbers for measles, mumps, and rubella. Although the mean population immunities for measles, mumps, and rubella were similar to the population-immunity thresholds, modelling for non-random mixing (unvaccinated children tend to

services; and the negative influence of so-called vaccine controversies in the media, especially the wider diffusion of vaccine-critical messages on the internet and social media. In most countries only a very small proportion of the population hold strong anti-vaccination convictions (so-called vaccine deniers). However, up to a third of people might have doubts and uncertainties that can lead them to refuse some vaccines but agree to others, delay vaccination, or follow the recommended schedule but with reluctance.[4]

Vaccine hesitancy, defined as delay in acceptance or refusal of vaccines despite availability of vaccination services, is now recognised as a complex and rapidly

Peter Dazeley/gettyimages

Lancet Infect Dis 2016

Published Online
February 4, 2016
http://dx.doi.org/10.1016/

Accompanied Comment (*Lancet Infectious Diseases*, 2016)

Managing the risk of vaccine hesitance and refusals

Comment

Sadly, putting Glasser and colleagues' recommended approach into practice remains easier said than done……

Transparent communications and tailored interventions can help to build trust in the effectiveness and safety of vaccines, in the system that delivers them, and in the motivations of the policy makers who decide which vaccines are needed when and where. This method takes commitment, but the tailored multipronged approach is the only way to maintain vaccination programme successes in the long run.

Peter Dazeley/gettyimages

for measles, mumps, and rubella were similar to the population-immunity thresholds, modelling for non-random mixing (unvaccinated children tend to

vaccine hesitancy, defined as delay in acceptance or refusal of vaccines despite availability of vaccination services, is now recognised as a complex and rapidly

Lancet Infect Dis 2016
Published Online
February 4, 2016
http://dx.doi.org/10.1016/

Mathematical models for within- and between-host dynamics IN ISOLATION

At individual level (cell-virus)

$$\frac{dT}{dt} = \Lambda - kVT - mT$$

$$\frac{dT^*}{dt} = kTV - (m+d)T^*$$

$$\frac{dV}{dt} = pT^* - cV$$

T, T^* Uninfected, Infected cells

V Density of virus

k Infection rate of cells

m, d Mortality of cells

p Virus production

c Clearance of viruses

$$\mathcal{R}_w = \frac{T_0 kp}{c(m+d)}$$

$\mathcal{R}_w$=1 is the threshold value.

At population level (an *SI* model)

$$\frac{dS}{dt} = b(N) - \lambda IS - \mu S$$

$$\frac{dI}{dt} = \lambda IS - (\mu + \delta)I$$

$$N = S + I$$

S, I Susceptible, Infected hosts

N Total density of hosts

λ Infection rate of hosts

b Birth rate of hosts

μ, δ Death rates of hosts

$$\mathcal{R}_b = \frac{\lambda N_0}{\mu + \delta}$$

$\mathcal{R}_b$=1 is the threshold value.

Coupling within- and between-host dynamics (nested models)

(Gilchrist & Sasaki, *JTB* 2002; **Gilchrist & Coombs, *TPB* 2006**; Boldin & Diekmann, *JMB*, 2008; Mideo, Alizon, & Day, *Trends Ecol Evol*. 2008; Qesmi, Heffernan & Wu, *JMB*, 2015)

At individual level (cell-virus)

$$\frac{dT}{dt} = \Lambda - kVT - mT$$

$$\frac{dT^*}{dt} = kTV - (m+d)T^*$$

$$\frac{dV}{dt} = pT^* - cV$$

T, T^* Uninfected, Infected cells

V Density of virus

k Infection rate of cells

m, d Mortality of cells, ***d* = *d*(*p*)**

p Virus production

c Clearance of viruses

$$\mathcal{R}_w = \frac{T_0 kp}{c[m + d(p)]}$$

At population level (*SI* model)

$$\frac{dS}{dt} = b(S,I) - \lambda(\hat{V})IS - \mu S$$

$$\frac{dI}{dt} = \lambda(\hat{V})IS - (\mu + \delta(\hat{T}))I$$

S, I Susceptible, Infected hosts

$\hat{T}, \hat{V}$ **Equilibrium values** (at fast time scale)

$b(S,I)$ Birth rate, $b(S_0, 0) = \mu N_0$

λ Infection rate of hosts

μ, δ Death rates of hosts

$$\mathcal{R}_b = \frac{\lambda N_0}{\mu + \delta} = \frac{\lambda(p) N_0}{\mu + \delta(p)}$$

Coupling within- and between-host dynamics (nested models)

(Gilchrist & Sasaki, *JTB* 2002; **Gilchrist & Coombs, *TPB* 2006**; Boldin & Diekmann, *JMB*, 2008; Mideo, Alizon, and Day, *Trends Ecol Evol*. 2008; Lenhart, 2014, 2015)

At individual level (cell-virus)

$$\frac{dT}{dt} = \Lambda - kVT - mT$$

$$\frac{dT^*}{dt} = kTV - (m+d)T^*$$

$$\frac{dV}{dt} = pT^* - cV$$

$$\mathcal{R}_w = \frac{T_0 kp}{c[m+d(p)]}$$

Let $\mathcal{R}_w(p^*) = \max_{0<p<p_{\max}} \mathcal{R}_w(p)$

At population level (*SI* model)

$$\frac{dS}{dt} = b(S,I) - \lambda(\hat{V})IS - \mu S$$

$$\frac{dI}{dt} = \lambda(\hat{V})IS - (\mu + \delta(\hat{T}))I$$

$$\mathcal{R}_b = \frac{\lambda(\hat{V})N_0}{\mu + \delta(\hat{T})} = \frac{\lambda_1(p)N_0}{\mu + \delta(p)}$$

Let $\mathcal{R}_b(p^\circ) = \max_{0<p<p_{\max}} \mathcal{R}_b(p)$

- If $p^*=p^\circ$, then there is no conflict between selection at the two different levels
- Otherwise, **a conflict exists** between natural selection at the two levels

Emerging disease dynamics

when the within- and between-host systems are

coupled dynamically

A project developed during a working group at NIMBioS

(Multi-scale Modeling of the Life Cycle of *Toxoplasma gondii*)

Life cycle of *Toxoplasma gondii*

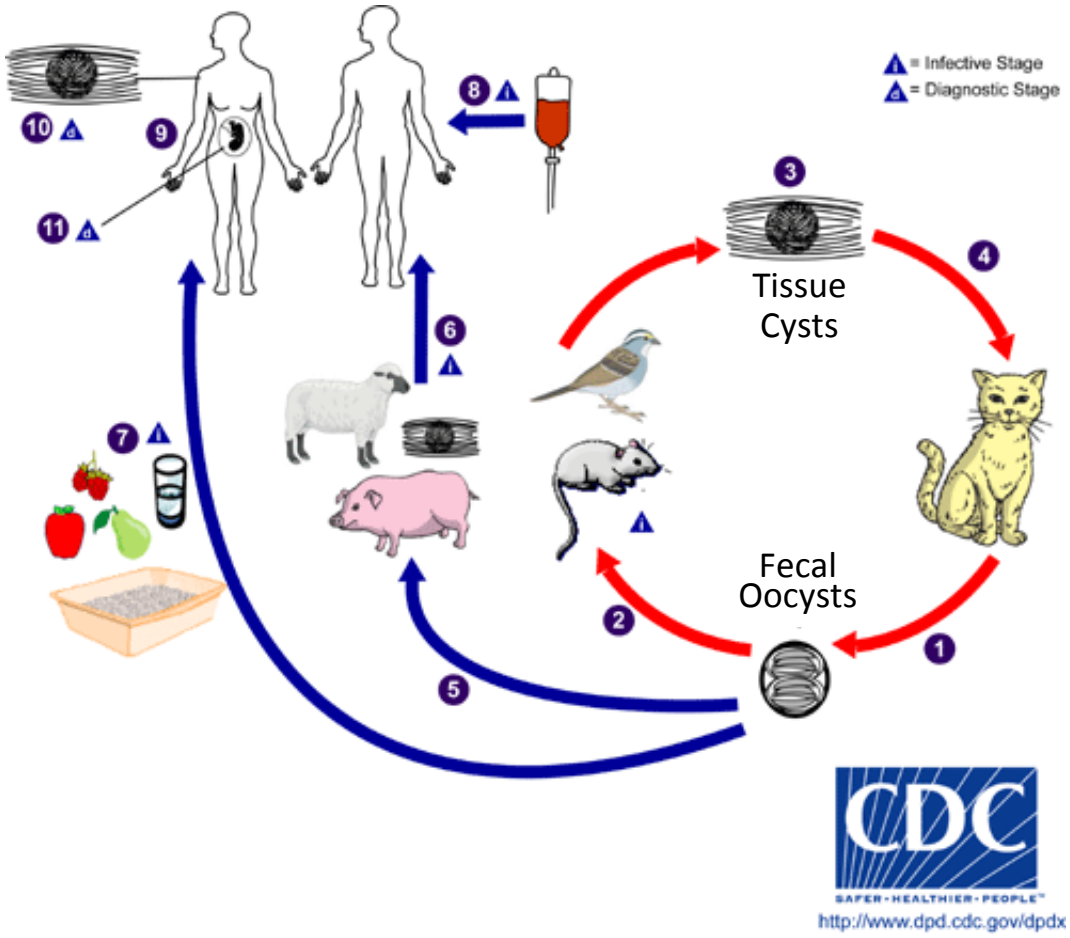

- The only known definitive hosts for *T. gondii* are members of family Felidae (domestic cats and relatives)
- Cats become infected after consuming infected rats, or directly by ingestion of sporulated oocysts, which can survive and remain infective for many months
- The parasites infect intestinal epithelial cells in cats. Tachyzoites invade cells and multiplies. When the cells die, the tachyzoites are released and infect other cells

Life cycle of *Toxoplasma gondii*

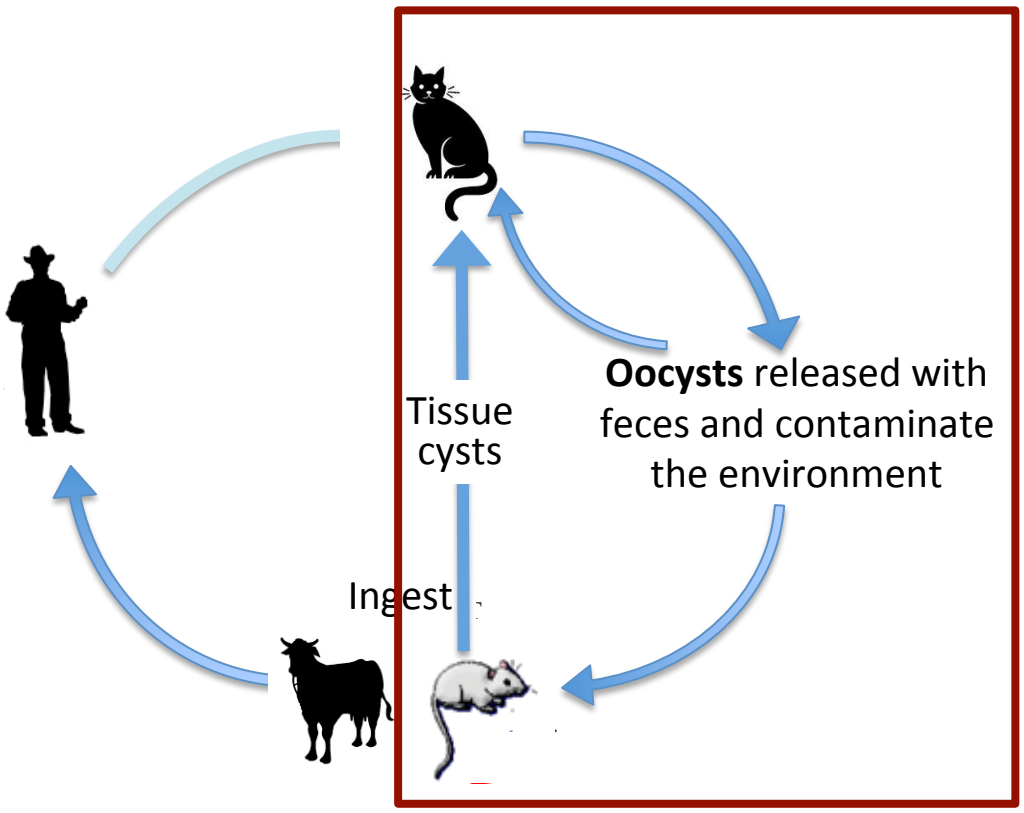

- The only known definitive hosts for *T. gondii* are members of family Felidae (domestic cats and relatives)
- Cats become infected after consuming infected rats, or directly by ingestion of sporulated oocysts, which can survive and remain infective for many months
- The parasites infect intestinal epithelial cells in cats. Tachyzoites invade cells and multiplies. When the cells die, the tachyzoites are released and infect other cells

Cellular stages of *T. gondii* (simplified)

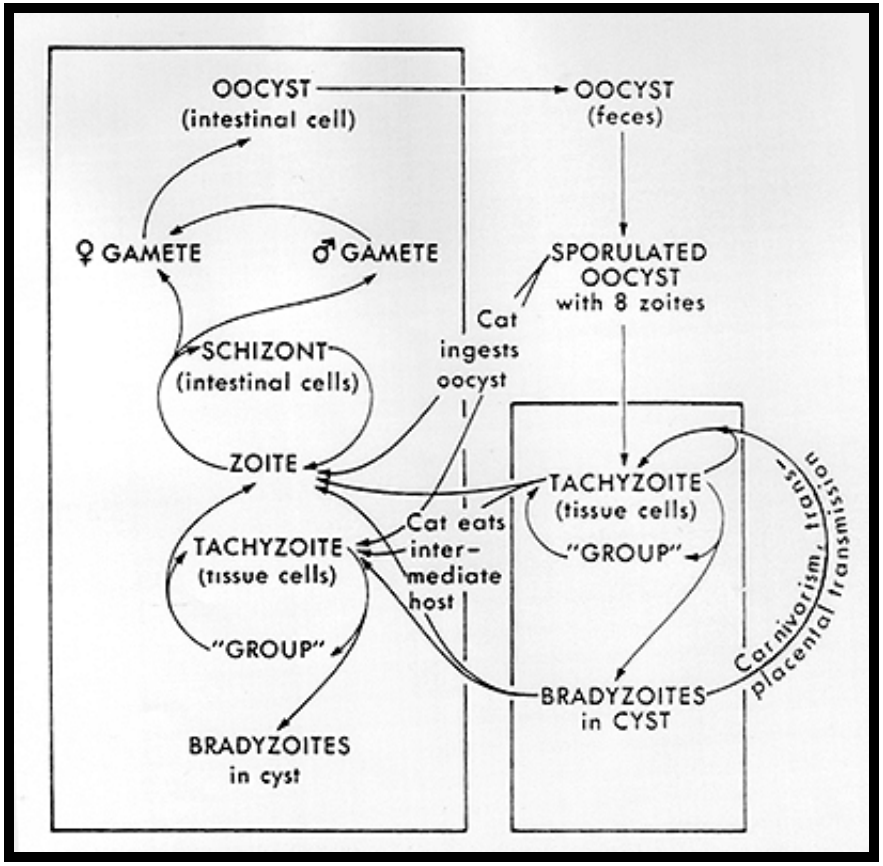

Illustration from: Georges' Parasitology for Veterinarians, 6th edition, D.D. Bowman, 1995. W.B. Saunders Co., Philadelphia, PA

A model dynamically coupling within- and between-host systems

- Z. Feng, J. Velasco-Hernandez, B. Tapia-Santos,
  A mathematical model for coupling within-host and between-host dynamics in an environmentally-driven infectious disease, *Mathematical Biosciences,* 2013

- X. Cen, Z. Feng, Y. Zhao,
  Emerging disease dynamics in a model coupling within-host and between-host systems, *J. Theoretical Biology*, 2014

- Z. Feng, X. Cen, Y. Zhao, J. Velasco-Hernandez,
  Coupled within-host and between-host dynamics and evolution of virulence, *Mathematical Biosciences*, 2015

A model dynamically coupling within- and between-host systems

Within-host sub-system:

$$\frac{dT}{dt} = \Lambda - kVT - mT$$

$$\frac{dT^*}{dt} = kTV - (m+d)T^* \qquad (1)$$

$$\frac{dV}{dt} = g(E) + pT^* - cV$$

Between-host sub-system:

$$\frac{dS}{dt} = \mu N - \lambda E S - \mu S$$

$$\frac{dI}{dt} = \lambda E S - \mu I \qquad (2a)$$

$$N = S + I \quad \text{(constant)}$$

Environmental contamination:

$$\frac{dE}{dt} = \theta I V (1 - E) - \gamma E \qquad (2b)$$

λ, k Transmission rates

μ Birth and death rate of hosts

m, d Mortality of cells

p Parasite production

c Mortality of parasites

θ, γ Contamination, clearance

$g(E)$ Ingestion of oocysts

$$g(0) = 0,\ g(E) \geq 0,\ g'(E) \geq 0,\ g''(E) \leq 0.$$

S, I Susceptible, Infectious hosts

E Environmental contamination ($0 \leq E < 1$)

T, T^* Uninfected, Infected cells

V Parasite density

The fast system for within-host dynamics

Consider the within-host **sub-system (1)** as the fast-system (**with E being constant**).

The within-host reproduction number: $\mathcal{R}_w = \dfrac{T_0 kp}{c(m+d)}$

Equilibrium for $E > 0$: for all $\mathcal{R}_w > 0$, there is a unique interior equilibrium given by $\tilde{U}(E) = \left(\tilde{T}(E), \tilde{T}^*(E), \tilde{V}(E)\right)$ where

$$\tilde{V}(E) = \frac{1}{c}\left(g(E) + p\tilde{T}^*(E)\right), \quad \tilde{T}^*(E) = \frac{m}{m+d}\left(T_0 - \tilde{T}(E)\right), \quad \tilde{T}(E) = \frac{1}{2}\left(a_1 - \sqrt{a_1^2 - 4a_2}\right) \tag{3}$$

with $a_1 = \dfrac{g(E)(m+d)}{pm} + T_0\left(1 + \dfrac{1}{\mathcal{R}_w}\right)$, $a_2 = \dfrac{T_0^2}{\mathcal{R}_w}$, $a_1^2 - 4a_2 \geq T_0^2\left(1 - \dfrac{1}{\mathcal{R}_w}\right)^2$.

Note: $\tilde{V}(E)$ provides an input for the between-host (I,E) sub-system.

Stability of the fast system

In the case when $g(E) = 0$, the global stability of (generalized) system (1) has been shown in P. De Leenheer and H. Smith (*SIAM J. Appl. Math.*, 2003)

Let $g(E)$ be any function satisfying the conditions:

$$g(0) = 0, \quad g(E) \geq 0, \quad g'(E) \geq 0, \quad g''(E) \leq 0.$$

Result 1. For $0 < E < 1$, the unique positive equilibrium of the fast system, $\tilde{U}(E) = \left(\tilde{T}(E), \tilde{T}^*(E), \tilde{V}(E)\right)$, is a **global attractor** for all $\mathcal{R}_w > 0$.

Moreover, the parasite load at the initial stage of environmental contamination is

$$\tilde{V}(0) = \lim_{E \to 0} \tilde{V}(E) = \begin{cases} 0 & \text{for } \mathcal{R}_w \leq 1, \\ \dfrac{m(\mathcal{R}_w - 1)}{k} & \text{for } \mathcal{R}_w > 1. \end{cases}$$

The sub-system on the slower time scale

The slow system consists of the between-host equations (2a) together with the environmental contamination equation (2b) with V being replaced by $\tilde{V}(E)$ of the positive equilibrium $\tilde{U}(E)=(\tilde{T}(E),\tilde{T}^{*}(E),\tilde{V}(E))$ of the fast system. That is:

$$\dot{I}=\lambda E(N-I)-\mu I, \qquad \dot{E}=\theta I\tilde{V}(E)(1-E)-\gamma E \tag{4}$$

The **between-host reproduction number** is:

$$\mathcal{R}_b=\frac{\theta\tilde{V}(0)}{\mu}\frac{\lambda N}{\gamma}$$

where $\tilde{V}(0)=\dfrac{m(\mathcal{R}_w-1)}{k}$ for $\mathcal{R}_w>1$

Result 2. Assume $\mathcal{R}_w>1$. The **infection-free** equilibrium $\boldsymbol{W_0}$**=(0,0)** is l.a.s. if $\mathcal{R}_b<1$ and unstable if $\mathcal{R}_b>1$.

Multiple positive equilibria of the slow system when $\mathcal{R}_b < 1$

Let $W^*=(I^*, E^*)$ denote an equilibrium of system (4) with $I^*, E^* > 0$. Then $I^* = \dfrac{\lambda E^* N}{\lambda E^* + \mu}$

and E^* satisfies the equation $F(E) = G(E)$ or $H(E) = F(E) - G(E) = 0$ where

$$F(E) = \frac{1-E}{c}\left[g(E) + \frac{pm}{m+d}\left(T_0 - \tilde{T}(E, \mathcal{R}_w)\right)\right], \qquad G(E) = \frac{\gamma E}{\theta N} + \frac{m(\mathcal{R}_w - 1)}{k\mathcal{R}_b}$$

$$\tilde{T}(E) = \frac{1}{2}\left(a_1 - \sqrt{a_1^2 - 4a_2}\right)$$

with $\quad a_1 = \dfrac{g(E)(m+d)}{pm} + T_0\left(1 + \dfrac{1}{\mathcal{R}_w}\right), \quad a_2 = \dfrac{T_0^2}{\mathcal{R}_w}$

Multiple positive equilibria of the slow system when $\mathcal{R}_b < 1$

Let $W^*=(I^*, E^*)$ denote an equilibrium of system (4) with $I^*, E^* > 0$. Then $I^* = \dfrac{\lambda E^* N}{\lambda E^* + \mu}$

and E^* satisfies the equation $F(E) = G(E)$ or $H(E) = F(E) - G(E) = 0$ where

$$F(E) = \frac{1-E}{c}\left[g(E) + \frac{pm}{m+d}\left(T_0 - \tilde{T}(E, \mathcal{R}_w)\right)\right], \qquad G(E) = \frac{\gamma E}{\theta N} + \frac{m(\mathcal{R}_w - 1)}{k\mathcal{R}_b}$$

$H(E)$ has the properties:

$$H(0)\begin{cases} = \tilde{V}(0)\left(1 - \dfrac{1}{\mathcal{R}_b}\right), & \text{if } \mathcal{R}_w > 1, \\ < 0, & \text{if } \mathcal{R}_w \le 1, \end{cases}$$

$H(1) < 0$ and $H''(E) < 0$.

Thus, it suffices to check the sign of

$$H_{\max} = \max_{0 \le E \le 1} H(E)$$

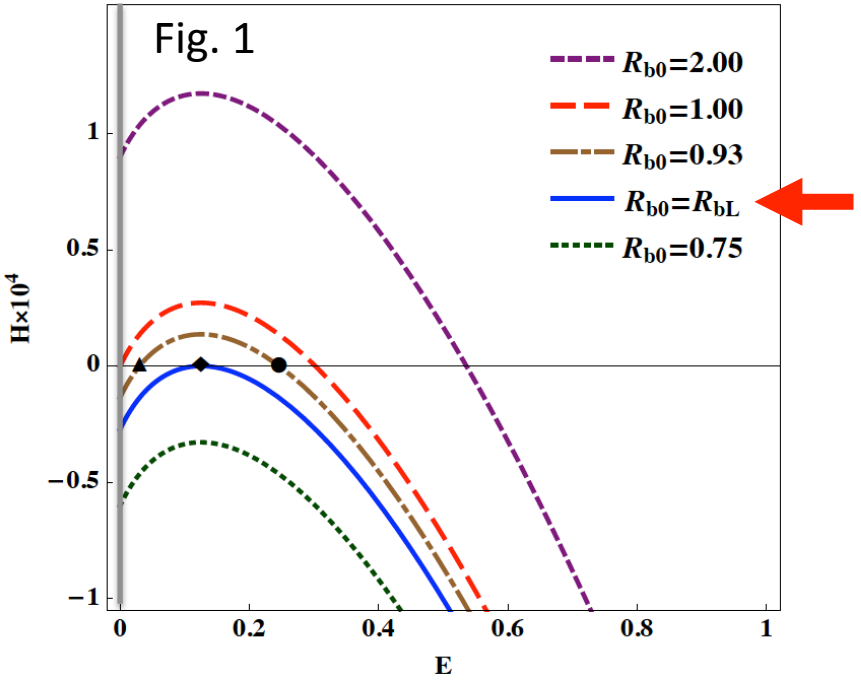

Multiple positive equilibria of the slow system when $\mathcal{R}_b < 1$

Let $E_1^* \le E_2^*$ denote the two possible roots of $H(E)$ and let $W_i^* = (I_i^*, E_i^*)$ denote the corresponding equilibria $(i = 1,\ 2)$. Denote $H_{\max} = \max_{0 \le E \le 1} H(E)$.

Result 3. (a) For $\mathcal{R}_w > 1$ and $\mathcal{R}_b > 1$, a unique $W^*=(I^*, E^*)$ exists.

(b) For $\mathcal{R}_w > 1$ and $\mathcal{R}_b < 1$,

(i) if $H_{\max} > 0$ then $W_1^* \ne W_2^*$ exist;

(ii) if $H_{\max} = 0$ then a unique $W^* = W_1^* = W_2^*$ exists;

(iii) if $H_{\max} < 0$ then W^* does not exist.

(c) For $\mathcal{R}_v < 1$, ……

Stability of equilibria for the slow system

Result 4. Existence and stability of interior equilibria of the slow system

Conditions			Existence and stability
$\mathcal{R}_w > 1$	$\mathcal{R}_b < 1$	$H_{\max} > 0$	W_1^* (unstab), W_2^* (l.a.s.)
		$H_{\max} = 0$	$W_1^* = W_2^*$ (saddle node)
		$H_{\max} < 0$	None
	$\mathcal{R}_b > 1$		Unique W^* (g.a.s.)

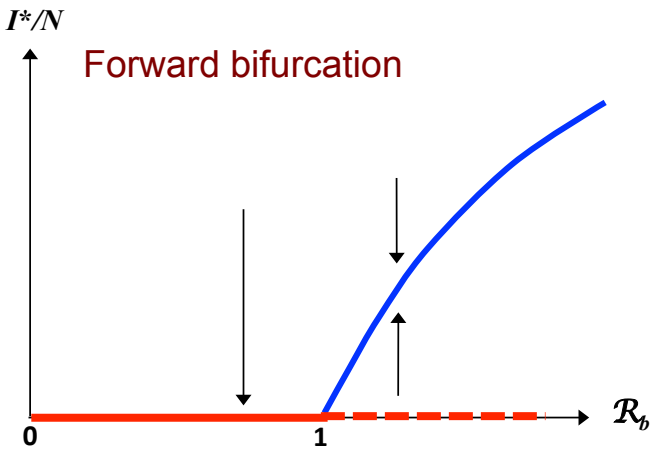

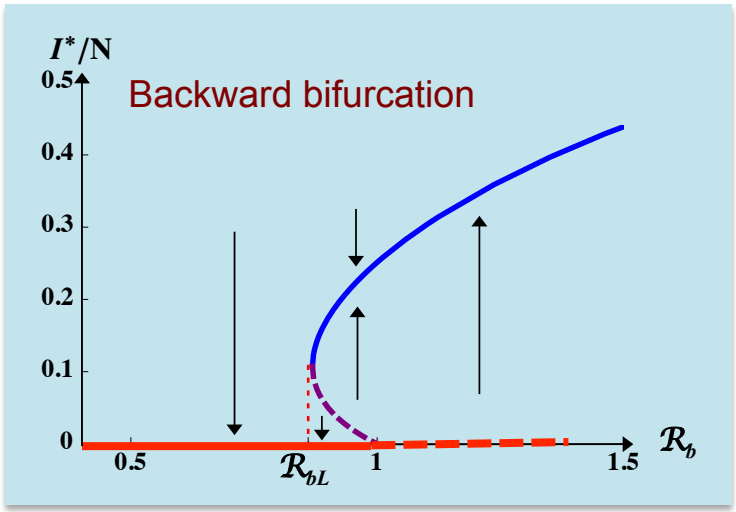

Fig. 2. Bifurcation diagrams for $\mathcal{R}_w > 1$

Numerical simulations of the full system (1) and (2)

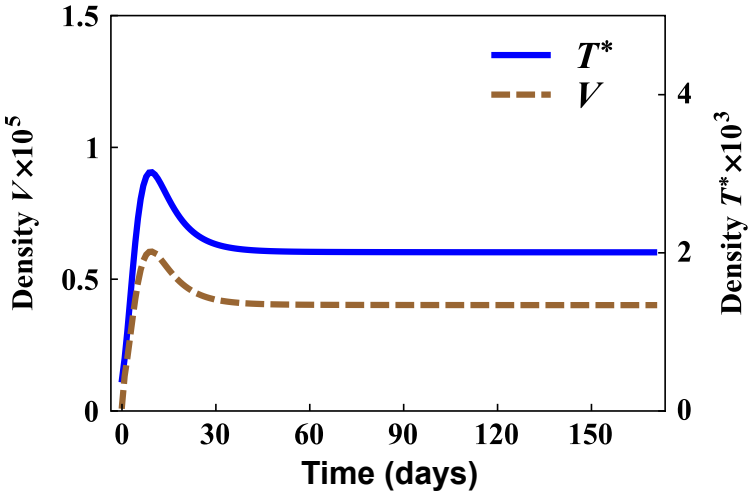

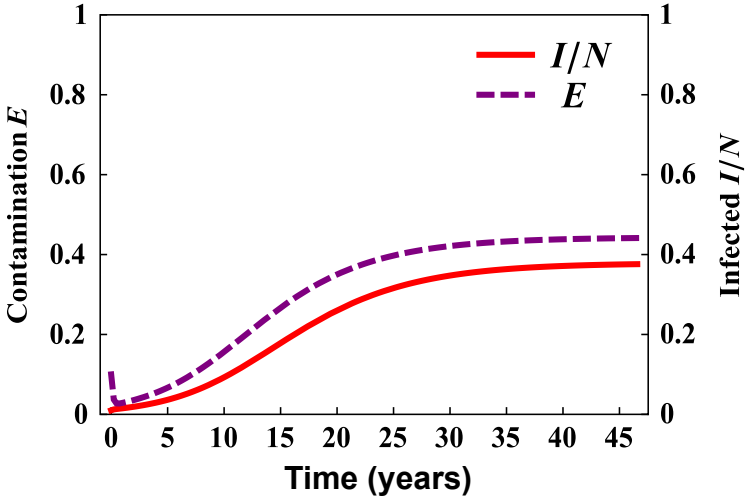

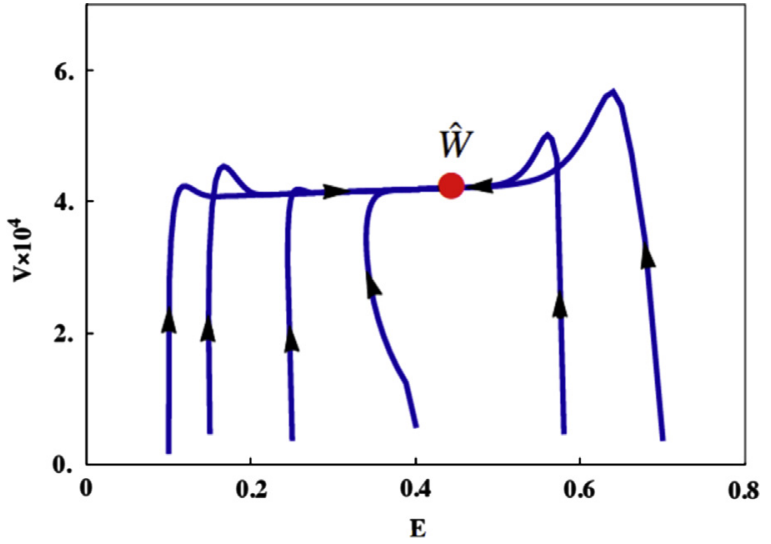

Fig. 3. Simulations of the coupled system showing dynamical behaviors of the fast and slow processes for the case $\mathcal{R}_w > 1$ and $\mathcal{R}_b > 1$ (there is a **unique** positive equilibrium $\hat{w}$).

Numerical simulations of the full system (1) and (2)

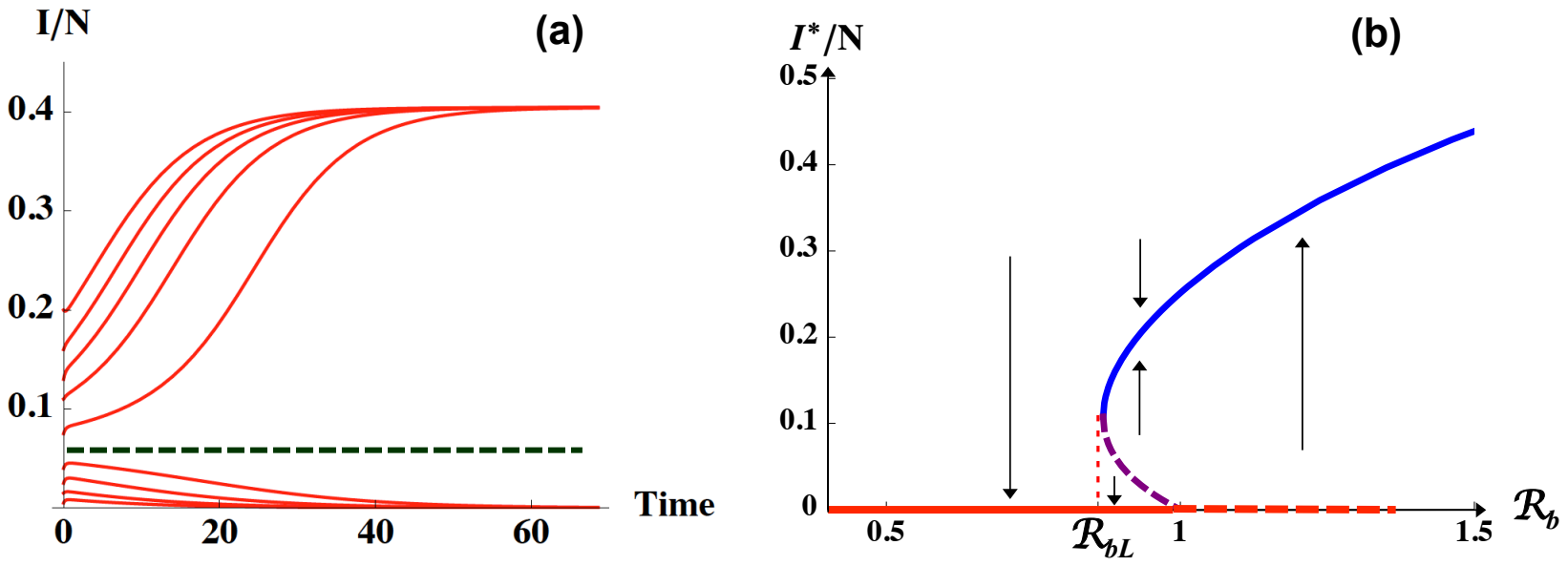

Fig. 4. **(a)** Simulations of the coupled system showing multiple stable equilibria for the case $\mathcal{R}_w > 1$ and $\mathcal{R}_b < 1$ (there are **two positive equilibria**). Plot **(b)** illustrates the lower bound of the window for the backward bifurcation.

The role of ingestion rate *a=g'(0)* in the backward bifurcation

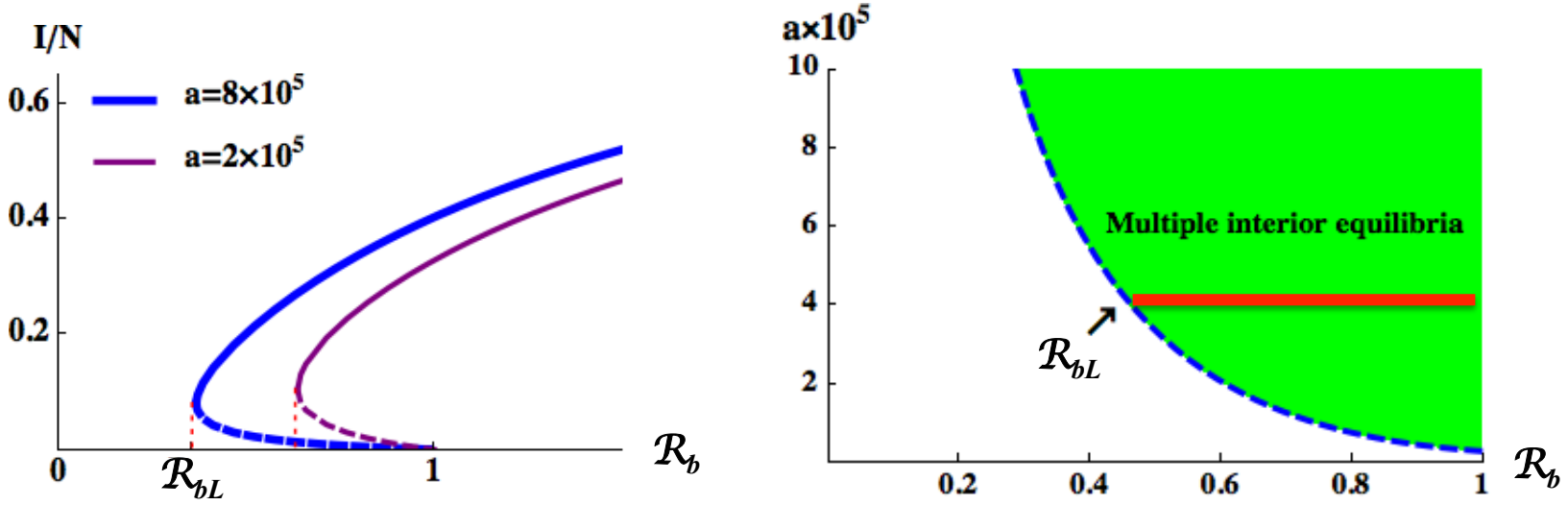

Fig. 5. The window for multiple interior equilibria, $(\mathcal{R}_{bL},1)$, increases with *a*.

Recall

$$\frac{dT}{dt} = \Lambda - kVT - mT$$

$$\frac{dT^*}{dt} = kTV - (m+d)T^*$$

$$\frac{dV}{dt} = g(E) + pT^* - cV$$

$$g(0)=0,\ \ g(E)\geq 0,\ \ g'(E)\geq 0,\ \ g''(E)\leq 0.$$

Examples:

1) $g(E) = aE$

2) $g(E) = \dfrac{aE}{1+bE}$

Evolution of virulence

Z. Feng, X. Cen, Y. Zhao, J. Velasco-Hernandez, *Math. Biosci.*, 2015

Within-host sub-system:

$$\frac{dT}{dt} = \Lambda - kVT - mT$$

$$\frac{dT^*}{dt} = kTV - (m+d)T^* \qquad (1)$$

$$\frac{dV}{dt} = g(E) + pT^* - cV$$

At steady-state:

$$\hat{V} = \frac{\Lambda_c p}{c(m+d)} - \frac{m}{k}, \quad \hat{T} = \frac{c(m+d)}{kp}$$

Between-host sub-system:

$$\frac{dS}{dt} = \mu N - \lambda ES - \mu S$$

$$\frac{dI}{dt} = \lambda ES - (\mu + \delta)I \qquad (2a)$$

$$N = S + I$$

Environmental contamination:

$$\frac{dE}{dt} = \theta(V)I(1-E) - \gamma E \qquad (2b)$$

Trade-off relationship (between transmission and pathogen virulence)

$$\theta(\hat{V}) = a_1 \hat{V}^z,\ z > 0 \quad \text{and} \quad \delta(\hat{T}) = a_2\left(\frac{1}{\hat{T}} - \frac{1}{T_0}\right)$$

Within-host and between-host fitness of pathogen

Burst size $\Phi(p) = \dfrac{p}{m + d(p)}$

Within-host RN $\mathcal{R}_w(p) = \dfrac{\Phi(p) k T_0}{c}$

Between-host RN $\mathcal{R}_b(p) = \dfrac{\theta(\hat{V}(p))}{\mu + \delta(\hat{T}(p))} \cdot \dfrac{\lambda S_0}{\gamma}$

where $\hat{V}$ and $\hat{T}$ are steady-state values of the within-host system

$$\hat{V}(p) = \frac{\Lambda_c \Phi(p)}{c} - \frac{m}{k}, \quad \hat{T}(p) = \frac{c}{k\Phi(p)}, \quad d(p) = d_0 p^2 \tag{5}$$

Let $\mathcal{R}_w(p^*) = \max\limits_{0<p<p_{\max}} \mathcal{R}_w(p)$ and $\mathcal{R}_b(p^\bullet) = \max\limits_{0<p<p_{\max}} \mathcal{R}_b(p)$

Relationship between virulence δ and pathogen production p

From $\delta(\hat{T}) = a_2\left(\frac{1}{\hat{T}} - \frac{1}{T_0}\right)$ and $\hat{T}(p) = \frac{c}{k\Phi(p)}$ $\Rightarrow$ $\delta(p) = a_2\left(\frac{k\Phi(p)}{c} - \frac{m}{\Lambda_c}\right)$

$$p^* = \min\{p_{\max}, p_c\}, \quad \delta^* = \delta(p^*) = \delta_{\max} \tag{6}$$

Notation:

- $p_{\max}$ -- Physiological upper bound for pathogen production
- p^* -- Optimal pathogen production at within-host level, $\mathcal{R}_w(p^*) = \max_{0<p<p_{\max}} \mathcal{R}_w(p)$
- p_c -- The critical point at which $\Phi'(p_c) = 0$ (or $\mathcal{R}_w'(p_c) = 0$)
- $p^\bullet$ -- Optimal pathogen production at between-host level $\mathcal{R}_b(p^\bullet) = \max_{0<p<p_{\max}} \mathcal{R}_b(p)$
- $\delta_{\max}$ -- Upper bound for virulence
- δ^* -- Optimal pathogen virulence at within-host level $\mathcal{R}_w(\delta^*) = \max_{0<\delta<\delta_{\max}} \mathcal{R}_w(\delta)$
- δ_c -- The critical point at which $\mathcal{R}_b'(\delta_c) = 0$
- $\delta^\bullet$ -- Optimal pathogen virulence at between-host level $\mathcal{R}_b(\delta^\bullet) = \max_{0<\delta<\delta_{\max}} \mathcal{R}_b(\delta)$

Optimal pathogen production p^* and $p^\bullet$ and virulence δ^* and $\delta^\bullet$

At the **between-host** level, consider the case z <1. Note that (see (5))

$$\theta(p)=a_1\left(\frac{\Lambda_c\Phi(p)}{c}-\frac{m}{k}\right)^z, \quad \delta(p)=a_2\left(\frac{k\Phi(p)}{c}-\frac{m}{\Lambda_c}\right)$$

Then θ can be written as a function of δ with $\theta(\delta)=\theta_0\left(\frac{\Lambda_c\delta}{a_2k}\right)^z$; and thus,

$$\mathcal{R}_b(\delta)=\frac{\lambda S_0\theta_0}{\gamma(\mu+\delta)}\left(\frac{\Lambda_c\delta}{a_2k}\right)^z, \quad \mathcal{R}_b(p)=\frac{\lambda S_0\theta_0}{\gamma(\mu+\delta(p))}\left(\frac{\Lambda_c\delta(p)}{a_2k}\right)^z \qquad (7)$$

Optimal pathogen production p^* and $p^\bullet$ and virulence δ^* and $\delta^\bullet$

Consider $\mathcal{R}_b(\delta) = \dfrac{\lambda S_0 \theta_0}{\gamma(\mu+\delta)}\left(\dfrac{\Lambda_c \delta}{a_2 k}\right)^z$ and $\mathcal{R}_b(p) = \dfrac{\lambda S_0 \theta_0}{\gamma(\mu+\delta(p))}\left(\dfrac{\Lambda_c \delta(p)}{a_2 k}\right)^z$.

Note that $\mathcal{R}_b'(\delta_c) = 0$, where $\delta_c = \dfrac{z\mu}{1-z}$, and

$$\frac{d\mathcal{R}_b}{dp} = \frac{d\mathcal{R}_b}{d\delta}\frac{d\delta}{dp} = (\delta_c - \delta) q \frac{d\delta}{dp},$$

where $q = \dfrac{\lambda S_0 a_1 (1-z)}{\gamma \delta (\mu+\delta)^2}\left(\dfrac{\Lambda_c \delta}{a_2 k}\right)^z > 0.$

At the within- and between-host levels:

$\delta^* = \delta(p^*) = \delta_{\max}$ and $\delta^\bullet = \min\{\delta_{\max}, \delta_c\}$

- If $\delta_{\max} < \delta_c$ then $\delta^\bullet = \delta^*$, $p^\bullet = p^*$ (Fig. (a))
- If $\delta_{\max} > \delta_c$ then $\delta^\bullet < \delta^*$, $p^\bullet < p^*$ (Fig. (b))

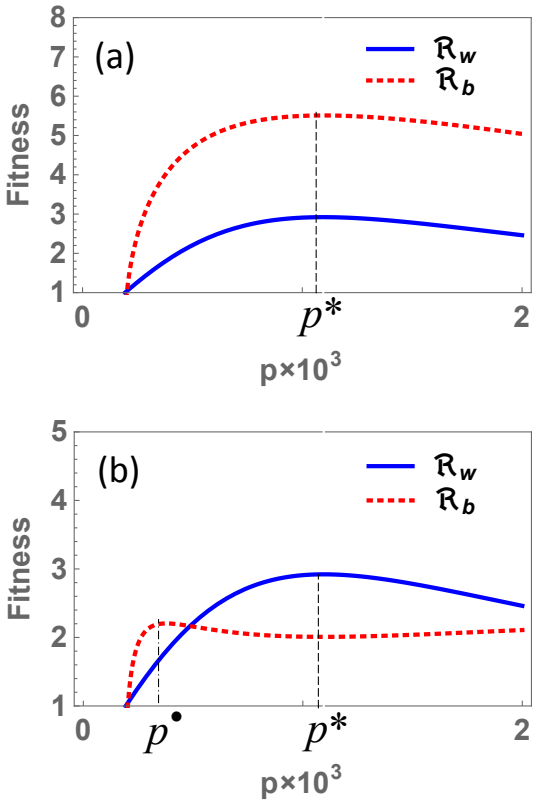

Summary

- When the within- and between-host systems are **in isolation**, the dynamics are determined by the reproduction numbers ($\mathcal{R}_w$ and $\mathcal{R}_b$) with **threshold equal to** 1.
- When the two systems are **dynamically linked**, backward bifurcations can occur, leading to a new threshold value $\mathcal{R}_b = \mathcal{R}_{bL} < 1$.
- Two time scales of the immunological and epidemiological processes allow the analysis of the **fast and slow systems** for the derivation of the threshold conditions. Numerical simulations of the full system confirms the analytic results.
- The window ($\mathcal{R}_{bL}$,1) for **multiple attractors** due to the backward bifurcation decreases with the inoculation rate constant ***a***, which can be reduced by control measures such as vaccination or reduced contact with contaminated environment
- The dynamically coupled model can be used to study questions related to **the evolution of pathogen virulence** and whether or not a conflict exists between natural selection at the within- and between-host levels.

Meta-population models and mixing: A case study

In 2000, authorities declared **measles** eliminated from the United States. In January 2008, **an intentionally unvaccinated** 7-year-old boy unknowingly infected with measles returned from Switzerland, resulting in the **largest outbreak** in San Diego, California, since 1991

Background

- Mathematical modeling has affected **vaccination policy** throughout the developed world and, via the WHO, elsewhere
- Policy goals vary with disease and setting, but **preventing outbreaks** is common
- This is attained by **exceeding the population immunity** at which $\mathcal{R}$, the average number of secondary infections per infectious person, is one
- The threshold (at which $\mathcal{R}_v$=1) is $p=1-1/\mathcal{R}_0$, where $\mathcal{R}_0$ is the average number of effective contacts while infectious

Background (cont'd)

- While immunity is at or above this threshold for many vaccine-preventable diseases in the US, policymakers are concerned about **heterogeneity** in vaccination coverage
- Socioeconomic status still affects access to medical care, but ACIP recommended vaccines became accessible in 1994 via the **Vaccines for Children Program**
- Currently, policymakers are concerned about **personal-belief exemptions (PBE)**, by which parents can avoid having their children vaccinated
- Parents who have the belief that vaccination is harmful tend to live in the same neighborhoods and, consequently, their children **attend the same elementary schools**

Personal belief exemption percentages by school and district, San Diego County

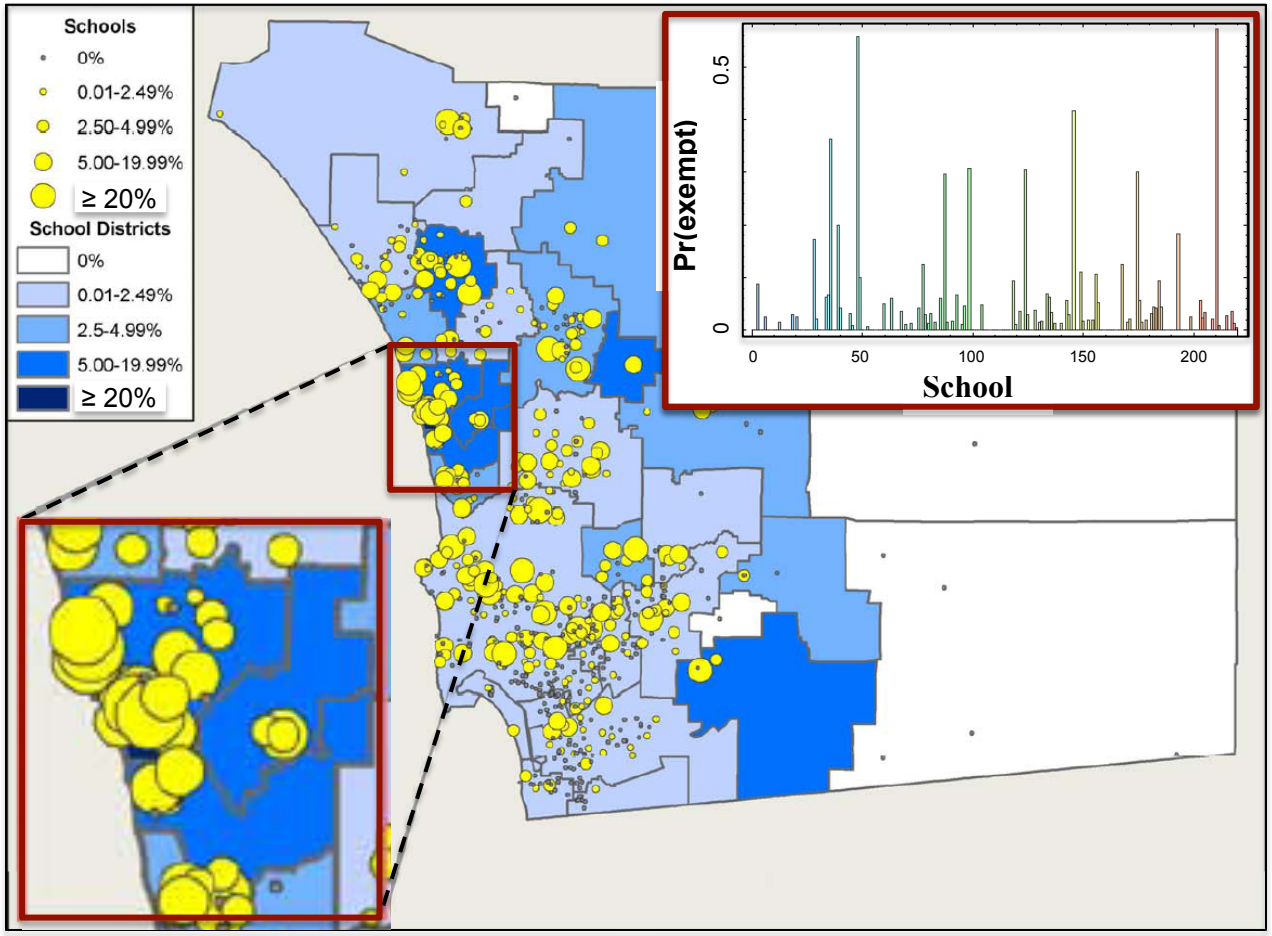

A metapopulation model and the mixing matrix (c_{ij})

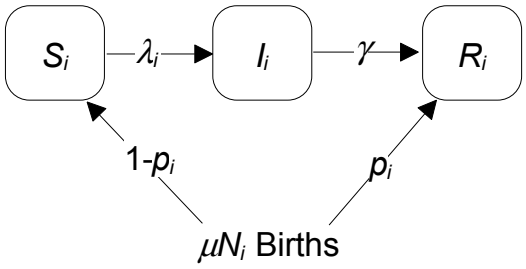

μN_i deaths omitted from the flow diagram

$$\frac{dS_i}{dt} = \mu N_i (1-p_i) - (\lambda_i + \mu) S_i$$

$$\frac{dI_i}{dt} = \lambda_i S_i - (\gamma + \mu) I_i$$

$$\frac{dR_i}{dt} = \mu N_i p_i + \gamma I_i - \mu R_i$$

$$\lambda_i = a_i \beta \sum_j c_{ij} \left(\frac{I_j}{N_j} \right)$$

$$N_i = S_i + I_i + R_i, \quad i, j = 1, \ldots, n$$

$$\Re_{vi} = \frac{(1-p_i)\beta a_i}{\gamma + \mu} = \Re_{0i}(1-p_i)$$

The next generation matrix is

$$K = \begin{bmatrix} \Re_{v1}c_{11} & \Re_{v1}c_{12} & \cdots & \Re_{v1}c_{1n} \\ \Re_{v2}c_{21} & \Re_{v2}c_{22} & \cdots & \Re_{v2}c_{2n} \\ \vdots & \vdots & \ddots & \vdots \\ \Re_{vn}c_{n1} & \Re_{vn}c_{n1} & \cdots & \Re_{vn}c_{nn} \end{bmatrix}$$

$\mathcal{R}_v = \rho(K)$ is the dominant eigenvalue of K

When n = 2,

$$\Re_v = \frac{1}{2}\left[A + D + \sqrt{(A-D)^2 + 4BC} \right], \text{ where}$$

$$A = \Re_{v1}c_{11},\ B = \Re_{v1}c_{12},\ C = \Re_{v2}c_{21},\ D = \Re_{v2}c_{22}$$

Baseline Characteristics

Table 1. Vaccination against measles, mumps and rubella in elementary schools in San Diego County, California.

Characteristic	Measles	Mumps	Rubella
$\mathcal{R}_0$ ignoring heterogeneity & mixing	**10.71**	8.49	4.08
Population-immunity threshold	0.907	0.882	0.755
Vaccine efficacy (dose 1) Vaccine efficacy (dose 2)	0.92 0.95	0.8 0.9	0.9 0.95
Average population immunity	0.922	0.872	0.921
$\mathcal{R}_0$ considering heterogeneity & non-random mixing	**18.06**	14.33	6.88
Population-immunity threshold	0.945	0.93	0.855
$\mathcal{R}_v$ considering heterogeneity & non-random mixing	3.39	2.88	1.29

Measles Results

Table 2. Impact of hypothetical interventions to control measles in San Diego County, California, elementary schools.

Intervention	Coverage	$\mathcal{R}_v$	Schools	Children
MMR coverage at school entry	97.1	3.39	638	39,132
Eliminating personal-belief exemptions	↑ 2.48	↓ **2.28**	292	972
Low-coverage, high-activity schools	↑ 0.4-0.9	↓ 0.24-1.37	65	164-342
All high-activity schools	↑ 0.9-1.4	↓ 0.26-1.37	385	369-547
All low-coverage schools	↑ 0.9-1.6	↓ **0.24-2.37**	114	361-638
Private schools	↑ 0.4	↓ 0.02	208	145

Among these interventions, eliminating non-medical exemptions is comparable to increasing by 50% the proportion of children vaccinated in low-coverage schools

Contributions of n=200 schools in San Diego District to $\mathcal{R}_0$ and $\mathcal{R}_v$ by location

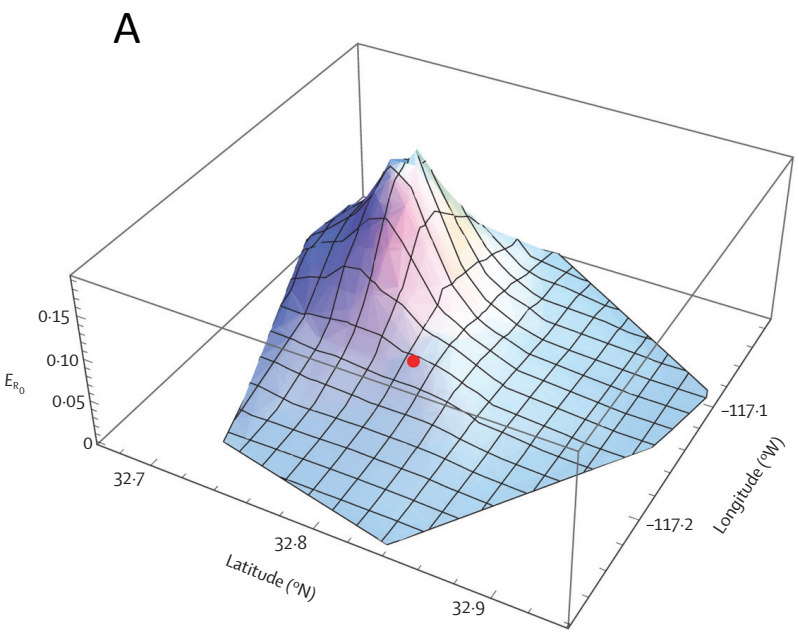

$\mathcal{R}_0$=13

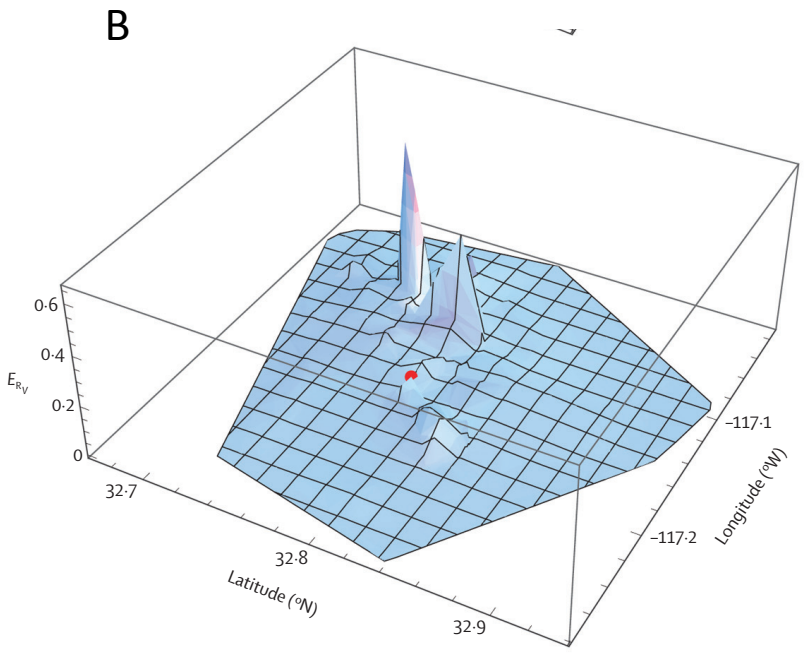

$\mathcal{R}_v$=1.3

Detailed results are presented in two published articles

- An elaboration of theory about preventing outbreaks in homogeneous populations to include heterogeneity or preferential mixing

  Zhilan Feng, Andrew Hill, Philip Smith and John Glasser
  J. Theoretical Biology, 2015

- The effect of heterogeneity in uptake of the measles, mumps, and rubella vaccine on the potential for outbreaks of measles: a modelling study

  John Glasser, Zhilan Feng, Saad Omer, Philip Smith, Lance Rodewald
  Lancet Infectious Diseases, 2016